JMATPRO	Journal of Advanced Materials and Processing 11 (3): 3-13, Summer 2023 https://sanad.iau.ir/journal/jmatpro Doi: 10.71670/jmatpro.2024.1106376

Research Paper

Effect of Aging on Microstructure and Tensile Properties of ASTM F75 Co-based Alloy Containing Different Carbon Contents

Shahin Torkamani, Masumeh Seifollahi*, Maryam Morakabati, Adli Akhondzadeh
Faculty of Materials and Manufacturing Technologies, Malek Ashtar University of Technology, Tehran, Iran

ARTICLE INFO

Article history:

Received 06 February 2024
Accepted 19 April 2024
Available online 1 August 2023

Keywords:
Co-Cr-Mo based alloy
aging
microstructure
carbide
tensile strength.

ABSTRACT

This study aims to investigate the effect of aging on microstructural evolution and mechanical properties of two ASTM F75 alloys, one without the carbon additive and the other one containing 0.21 wt.% C. Aging on the samples solution-annealed at 1225 °C for 1 hour was performed at 720, 760, and 800°C for 5 hours. The evaluation of the microstructure of both samples after aging showed that the γ→ε transformation led to the formation of two various morphologies of the precipitates in the regions of the ε-phase. At the first stages of aging, the precipitates appeared as a series of straight bands in both samples, while with an increase in the temperature, pearlite-like regions were found at the grain boundaries of only the carbon-containing sample. In the sample without the carbon additive, the microstructure consisted of the σ-phase. In the carbon-containing sample, lamellar $M_{23}C_6$ carbides were formed during aging in the vicinity of the remaining blocky $M_{23}C_6$ carbides. The carbon-containing sample consisted of fine $M_{23}C_6$ carbides after aging at 720°C, which were distributed inside the grains and at the grain boundaries. The appropriate precipitation rate and their optimum distribution in the structure led to an increase in the yield strength by up to 15%, along with an increase in the ultimate tensile strength by up to 6% compared with the as-cast state. However, no significant improvement was found in the ductility of the alloy.

Citation: Torkamani, Sh.; Seifollahi, M.; Morakabati, M.; Akhondzadeh, A. (2023). Effect of Aging on Microstructure and Tensile Properties of ASTM F75 Co-based Alloy Containing Different Carbon Contents, Journal of Advanced Materials and Processing, 11 (3), 3-13. Doi: 10.71670/jmatpro.2024.1106376

* **Corresponding Author:**
E-Mail: m_seifollahi@mut.ac.ir

1. Introduction

Medical grade casting ASTM F75 alloy is based on 27-30 wt.% Cr, 5-7 wt.% Mo, and a balanced amount of Co, along with a minor content of other elements such as C, N, Si, Mn, Al, Ti, Fe, Ni, and B. This alloy is broadly employed to fabricate orthopedic implants owing to its high strength because of the formation of carbides and its high wear resistance [1-3].

ASTM F75 alloy (in as-cast/annealed conditions) is widely used in the fabrication of prosthetics due to its high corrosion resistance in body fluid environments. The characteristics of the ordinary casting process, such as large grain size and casting defects, lead to both low yield strength and fatigue fracture in the hip prosthesis area. Therefore, to overcome these problems, investment casting and powder metallurgy methods are suitable alternatives. The investment casting process is usually used to reduce the grain size and also to improve the distribution of alloying elements and carbides [4,5]. The defects formed in the as-cast condition have motivated researchers to study the effect of various heat treatments on the microstructure and mechanical properties of this alloy. Common heat treatments performed on this alloy include solution annealing and aging [6]. Controlling the carbon content of the solution, morphology, and the distribution of the carbides formed in the Co-Cr-Mo-based alloys are of great importance in enhancing the mechanical properties of these alloys [7,8].

The microstructure of ASTM F75 alloy in as-cast conditions, according to its chemical composition, can consist of matrix phases of γ from FCC cobalt or ε from HCP cobalt, $M_{23}C_6$ secondary carbides with blocky and lamellar morphologies, σ phase, and M_6C phase. The formation of $M_{23}C_6$ is considered the major strengthening mechanism in this alloy. The addition of carbon leads to an enhancement in both the stability of the γ-phase and mechanical properties. However, the addition of excess amounts of carbon causes the formation of $M_{23}C_6$ carbide [9-11]. When coarse $M_{23}C_6$ carbides are precipitated along the grain boundaries, they can act as preferred sites for the propagation of fatigue cracks. Therefore, obtaining an optimal microstructure through uniform distribution of precipitates, morphology, size, and volume fraction of these precipitates in the matrix phase is done to enhance the mechanical properties by the solution annealing heat treatment and aging [12]. Regarding their chemical composition, cobalt-chromium-molybdenum-based alloys possess two matrix phases, i.e., low-temperature ε with an HCP crystal structure and high-temperature γ with an FCC crystal structure. The γ→ε transformation temperature for pure Co is 417 °C. However, by adding elements such as Cr and Mo, the transformation temperature reaches 870 °C since these elements are ε-stabilizing elements [13]. The ε-phase resulting from the γ→ε transformation is known as the martensitic ε. The martensitic ε could be achieved in three ways: 1- Isothermal transformation, 2- Athermal transformation, and 3- Strain-induced transformation during the heat treatment [14].

Most of the studies on this subject investigated the effect of alloying elements such as Cr, N, Ni, Si, and Mn on the microstructure of ASTM F75 alloy, and only a few studies have paid attention to the microstructure and mechanical properties of the alloy, and the effect of heat treatments on the enhancement of mechanical properties has been rarely reported. Song Lee et al. [15] fabricated various samples of ASTM F75 alloy with various amounts of carbon from 0 to 0.18 wt.% and found an increase in the volume fraction of the γ-phase from 12 to 30. This led to an increase in the tensile strength and ductility (30%) with the presence of 0.1 wt.% C. In addition, carbon increased the stacking fault energy while decreasing the density of the stacking fault, which led to the stabilization of the γ-phase. In another study, Dobbs et al. [16] investigated the effect of the solution annealing heat treatment at 1240 °C (for 0.5, 1, 2, 4, and 8 hours) and aging at 720 °C (for 6, 9, 16, 24, 48 hours) on tensile properties. They showed that heat treatment, in general, causes an improvement in the mechanical properties without compromising corrosion resistance. Also, the optimal properties are achieved in the sample undergoing partial solution annealing (at 1225 °C for 15 min and air cooling). Herrera et al. [17] studied the effect of carbon content on the mechanical properties of ASTM F75 alloy in as-cast and solution-annealed conditions and fabricated three alloys with low, medium, and high amounts of carbon to evaluate the effect of carbon content. They found that carbon content exhibited a noticeable effect on the mechanical properties of the heat-treated alloys, and the alloy with a medium amount of carbon showed the most optimal mechanical properties.

This study aims to investigate the microstructural evolution of ASTM F75 alloy, with and without the carbon additive, by changing the heat treatment cycle of the solution annealing to compensate for the poor mechanical properties of this alloy, such as its low strength and ductility in the as-cast state.

2. Experimental procedure

The ingots with different amount of carbon were melted in an induction melting furnace under Ar inert gas and cast into a Al_2O_3 crucible. Cast ingots were annealed at 1225 °C for 1 h followed by water quenching. 10×10×10 mm samples were exposed to aging test in temperaturess of 720, 760 and 800 °C for 5 h and quenched into water. The electrical resistance furnaces used in this research had accuracy about ±5 °C. Chemical composition determined using quantometry method (Spectro2004) and the results are listed in table 1.

Table 1. Chemical composition of ingots in accordance to standard.

element	Co	Cr	Mo	Si	Mn	Fe	Al	C
ASTM F75 [18]	Bal.	27-30	5-7	<1	<1	<0.75	<0.1	<0.35
Product 1	Bal.	28.16	5.49	0.35	0.53	0.3	0.016	0.01
Product 2	Bal.	28.24	5.63	0.32	0.43	0.24	0.077	0.21

Metallographic sections were prepared using standard mechanical polishing procedures and elctroetched using 90% H2SO4-10% methanol solution for 30-240 second with the voltage of 6 Volt. A Vega Tescan scanning electron microscope (SEM) with an energy dispersive spectroscopy (EDS) analyser operating at 15 kV and optical microscopy (Olympus DP25) were used to observe the morphology and distribution of the phases.
A Rigaku Smart Lab XRD was used with Cu-Kα radiation at 40 kV and 30 mA. The volume fraction of phases was calculated by Imag J analysis software. Tensile tests at room-temperature were carried out on an Instron Model-8502 test machine. Tensile tests were conducted in accordance with ASTM E8 [19] of the tension testing of metallic material.

3. Results and Discussion

3.1. Microstructural investigations

Figures 1 and 2 present the optical micrographs of the samples with and without carbon in different annealing and aging conditions. In samples without carbon, some precipitates can be found, the EDS analysis of which is shown in Fig. 3 for the sample aged at 760 °C. As can be seen in point A, the matrix phase consists of the base alloy elements, i.e., Cr, Mo, and Co, with atomic percentages of 32.28, 67.77, and 2.95, respectively. In point B, Cr, Co, and Mo are present with atomic percentages of 42.97, 48.33, and 8.70. Thus, it appears that the precipitates present are of σ type. σ precipitates could also be found in annealed conditions, and with an increase in the aging temperature from 720 °C to 800 °C, the amount and size of σ precipitates increased. This can be explained by the fact that the aging temperature was close to the temperature range of the formation of σ, i.e., 540-980 °C [20]. σ exhibits a tetragonal structure, which is composed of the Co-Cr intermetallic phase. Due to its brittle nature, this phase is detrimental. By adding carbon, $M_{23}C_6$ carbides were formed, according to reports of other studies (Co-Cr/M) + C→ $M_{23}C_6$) [1], which can play a crucial role in precipitation strengthening.
The formation of $M_{23}C_6$ precipitates will be discussed in the carbon-containing alloy.

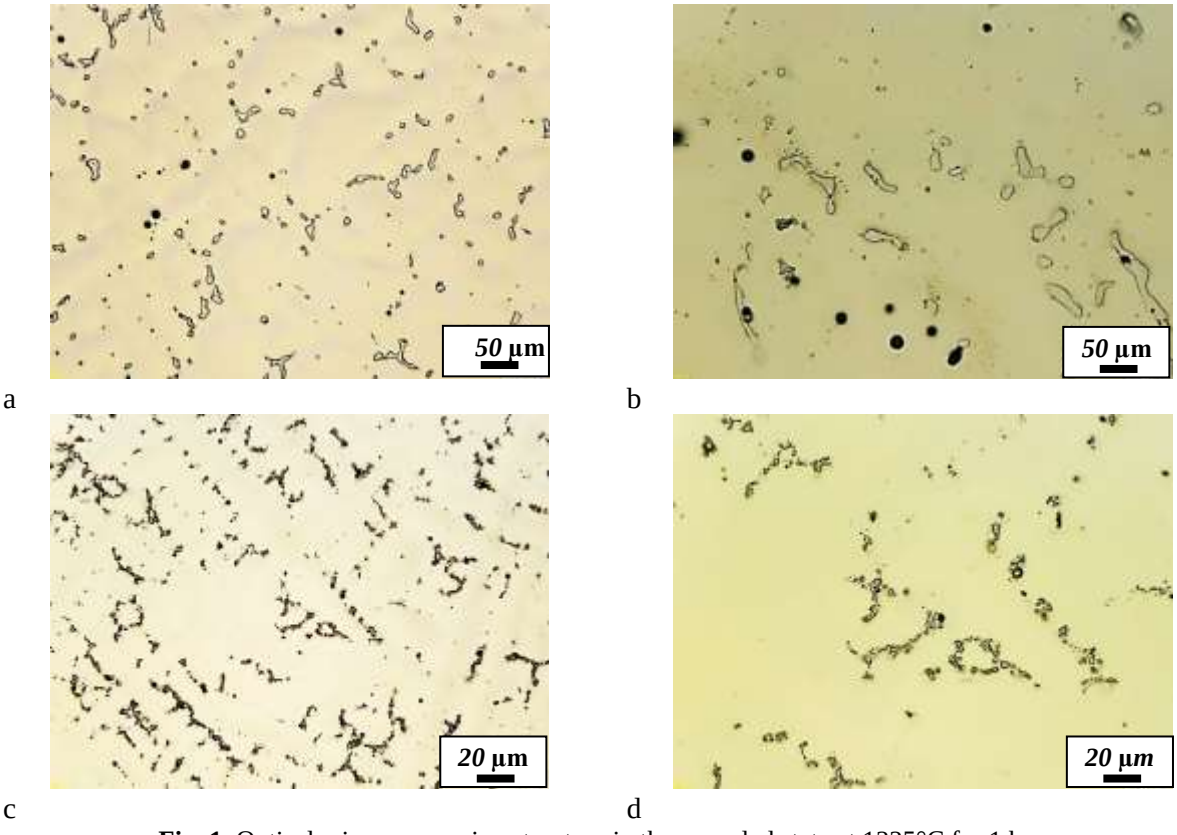

a b c d

Fig. 1. Optical microscope microstructure in the annealed state at 1225°C for 1 hour:
a,b) Samples without carbon c,d) Samples with carbon

At 800 °C and in the sample without the carbon additive, a series of precipitates were formed as straight bands around the initial precipitate of the σ-phase, which can be seen in the optical micrograph of Fig. 4 with a higher magnification. These regions are the ε-martensite phase with an HCP structure with numerous stacking faults, which are the preferred sites for the formation of precipitates. The reason for the formation of the precipitates in these regions is that Co present in the matrix reacted with Cr and Mo, which were segregated preferentially to dislocations and stacking faults, and the σ-phase was formed as straight bands.

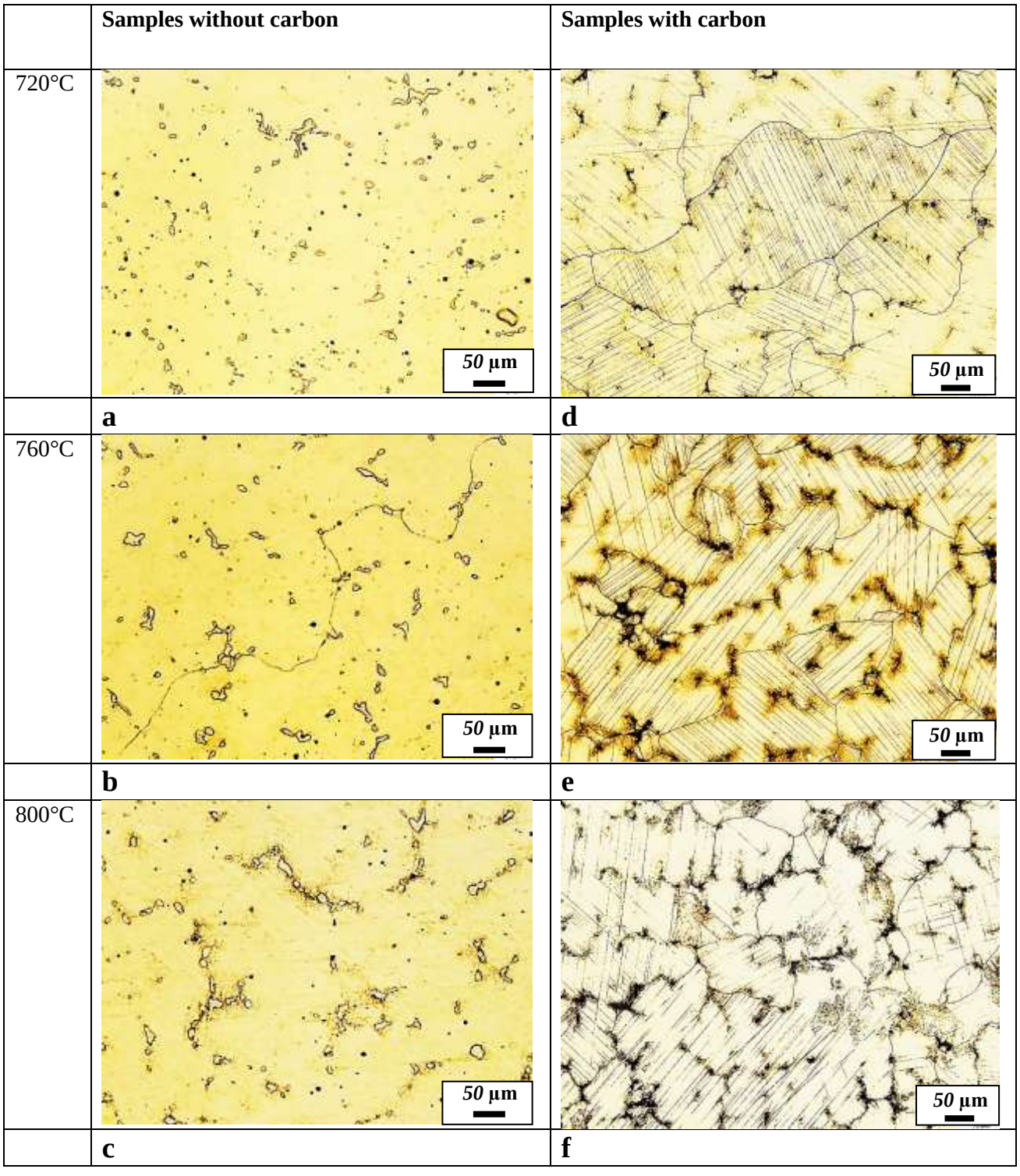

Fig. 2. Optical microstructure images of a, b, c) carbon-free and d, e, f) carbon-containing samples aged for 5 hours at temperatures of a,d) 720°C, b,e) 760°C, c,f) 800°C

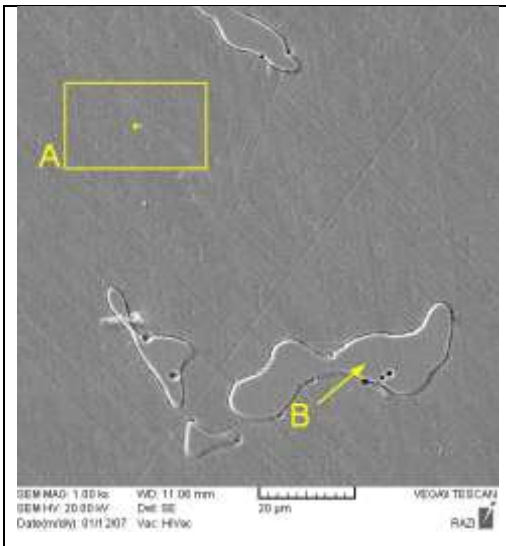

A			
Elements	Chromium	Cobalt	Molybdenum
At %	32.28	64.77	2.95
Wt %	29.04	66.06	4.90
B			
Elements	Chromium	Cobalt	Molybdenum
At %	42.97	48.33	8.70
Wt %	37.76	48.13	14.11

Fig. 3. The electron microscope image of the microstructure of the carbon-free sample aged at 760°C for 5 hours along with the results of EDS analysis

According to the literature [21,22], by aging at temperatures lower than 925 °C, two mechanisms can be proposed for the γ→ε transformation. The first one suggests that in the short times of the first stages of aging, the FCC to HCP_1 transformation with an orientation relationship of FCC{111} ‖ $_{HCP}$ {0001} leads to the formation of the ε-martensite. The regions of the FCC phase are single-phase, while those of the HCP phase consist of carbides, as well. These carbides exhibit an orientation relationship of $\{0001\}_{HCP} \parallel \{111\}_{M23C6}$ with HCP. Therefore, the carbide nucleation in HCP_1 occurs as a series of straight bands. The second mechanism, which was seen in the alloys that contain carbon, suggests that at longer times and higher aging temperatures, the FCC to HCP_2 transformation occurred at the grain boundaries from the FCC matrix along with the carbide nucleation and results in the formation of a lamellar pearlite-like morphology, which will be discussed in the following.

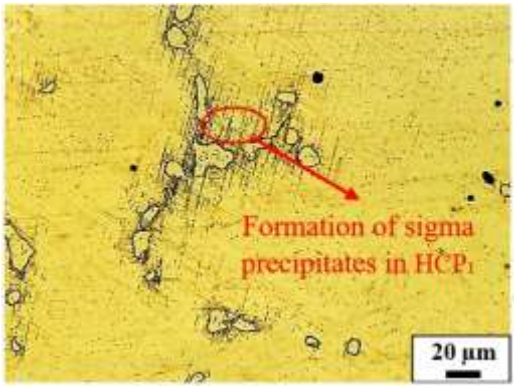

Fig. 4. Image of the optical microstructure of the carbon-free sample aged for 5 hours at 800°C

Figure 2d-f shows the microstructures of the carbon-containing sample aged at 720 °C, 760 °C, and 800 °C, which consist of fine $M_{23}C_6$ precipitates at the grain boundaries and inside the grains along with parallel lines of the precipitation of carbides in HCP_1. The scanning electron microscope (SEM) micrograph and the EDS analysis for the formation of $M_{23}C_6$ in the regions of HCP_1 in the sample aged at 760 °C are displayed in Fig. 6. According to the EDS analysis of point A in Fig. 6d, the concentration of Cr is higher than that of Co and Mo. Since the Cr content in $M_{23}C_6$ carbide has been reported to be higher than that of Co and Mo [17], it appears that this precipitate was of $M_{23}C_6$ type. The reason for the absence of the σ-phase precipitates in the carbon-containing sample, as stated previously, is that these precipitates reacted with carbon present in the alloy, and $M_{23}C_6$ carbides were formed. Since the stacking fault density in the HCP crystal structure is higher than that in the FCC crystal structure [23], the presence of the stacking fault in these regions led to a significant decrease in the activation energy of the

precipitation. The solute atoms present in the alloy, which were dissolved by solution annealing, had a strong tendency to segregate in these regions. Therefore, parallel lines were the preferred sites for the nucleation of $M_{23}C_6$ carbides. With an increase in the aging temperature to 760 °C, as shown in Fig. 2e, the precipitation rate of $M_{23}C_6$ carbides inside the grains and especially at the grain boundaries increased, and coarser precipitates could be found at this temperature compared with those at 760 °C. In addition, it can be seen that the γ→ε transformation has been done more at this aging temperature, and the parallel lines related to the precipitation of $M_{23}C_6$ carbides increased in the regions related to HCP_1. In the early stages of aging, especially at low temperatures and short times, the formation of precipitates often occurs in the form of parallel lines in HCP_1 regions, and the formation of carbides with a pearlite-like morphology occurs at higher temperatures and longer times.

The XRD pattern of the carbon-containing sample after aging is seen in Fig. 5. With an increase in the aging temperature from 720 °C to 760 °C in the aged samples, the peaks corresponding to the ε-phase increased due to the occurrence of the γ→ε transformation because of the increase in the stacking fault and distortion, whereas the peak corresponding to the γ-phase decreased.

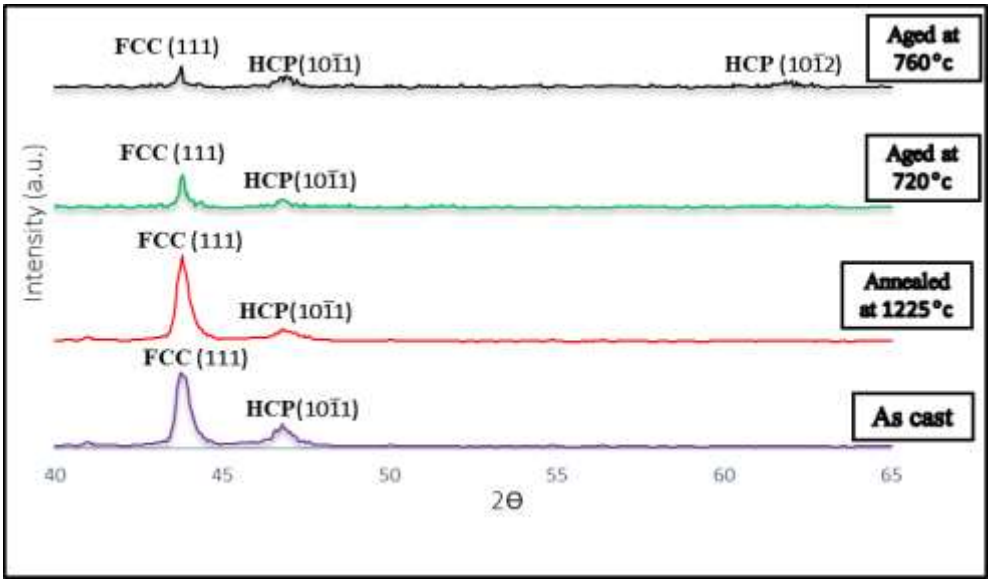

Fig. 5. X-ray diffraction pattern of ASTM F75 sample containing carbon in different conditions.

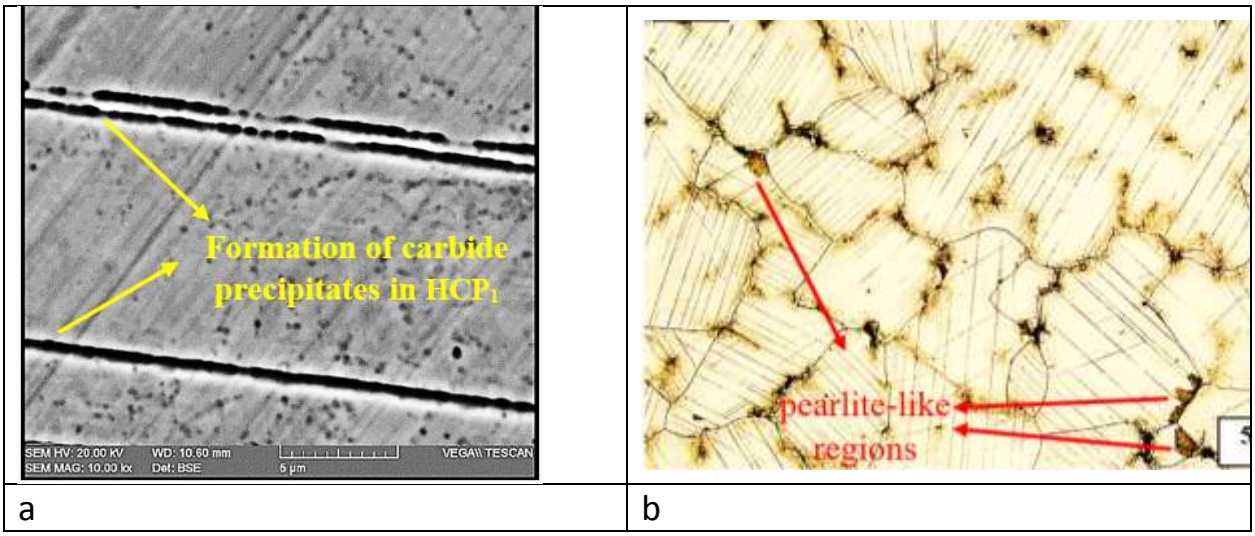

a b

	A	
Elements	At %	Wt %
Carbon	35.01	10.02
Chromium	21.53	26.69
Cobalt	38.97	54.76
Molybdenum	3.25	7.43

c d

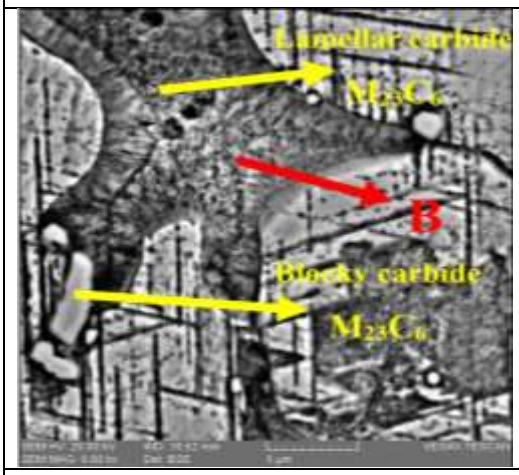

	B	
Elements	At %	Wt %
Carbon	43.56	13.25
Chromium	25.68	33.82
Cobalt	20.87	31.15
Molybdenum	8.34	20.25

e f

Fig. 6. Optical microstructure and electron microscope image of the sample containing carbon aged at 760°C for 5 hours with the results of EDS analysis.

It has been reported that [24] carbon atoms tend to be absorbed by dislocations and stacking faults and form segregated regions of carbon. These carbon atoms react with chromium and molybdenum atoms, which segregate preferentially to dislocations and stacking faults and lead to the creation of regions in the form of parallel lines. Another effect that was observed by adding carbon to ASTM F75 alloy aged at 760°C was the formation of a phase with a pearlite-like morphology at the grain boundaries. By increasing the aging temperature and time, the conditions for the transformation are provided in the form of a series of discontinuous reactions simultaneously with the formation of HCP_2 at the grain boundary, which has a low stacking fault, unlike HCP. This can be explained by the high mismatch at the grain boundaries and an increase in the growth rate of carbides in these regions due to an increase in the diffusion rate caused by increasing the aging temperature. The optical and SEM micrographs of the pearlite-like region formed at the grain boundaries can be seen in Fig. 6b and Fig. 6c, respectively. As shown, in the pearlite-like phase, the Co content is higher than that in the lamellar carbide, according to the EDS analysis result in Fig. 6d. The reason is that this region consisted of two phases, i.e., $M_{23}C_6$ and ε. The high content of Co in this region is related to the presence of the ε-martensite phase, which was formed from the γ→ε transformation during aging. Figure 6d shows $M_{23}C_6$ carbides with two different morphologies. In this figure, blocky carbides remaining from solution annealing can be observed around lamellar carbide (black) formed in the aging conditions. Due to the dissolution of a part of blocky carbides during solution annealing at 1225 °C for 1 hour, the content of C, Cr, and Mo around these carbides increased. During aging, lamellar carbides were formed because of appropriate conditions provided for the diffusion and segregation of the elements, which are seen in black color in the three microstructures aged at 720 °C, 760 °C, and 800 °C, similar to the lamellar carbides present in the as-

cast condition. With an increase in the aging temperature to 800 °C and according to Fig. 2f, an increase in the temperature led to the coarsening of lamellar $M_{23}C_6$ carbides and the formation of more consistent precipitates, especially at the grain boundaries. The morphologies observed at 720 °C as parallel lines and pearlite-like regions that appear at the grain boundaries became more prominent at this aging temperature (800°C).

According to Fig. 2f, lamellar $M_{23}C_6$ carbides (black regions) can be found inside the grains, especially at the grain boundaries. Another noteworthy point is that the volume fraction of the pearlite-like regions (gray regions) increased at the grain boundaries with an increase in the aging temperature compared with that of the samples aged at 720 and 760 °C since increasing the aging temperature led to an increase in the diffusion rate of the elements at the grain boundaries and as well as an increase in the mismatch of the grain boundaries. Also, the ε-martensite was formed with an increase in the stacking fault density.

3.3. Hardness measurements

Figure 7 presents the hardness values of the as-cast, annealed, and aged samples.

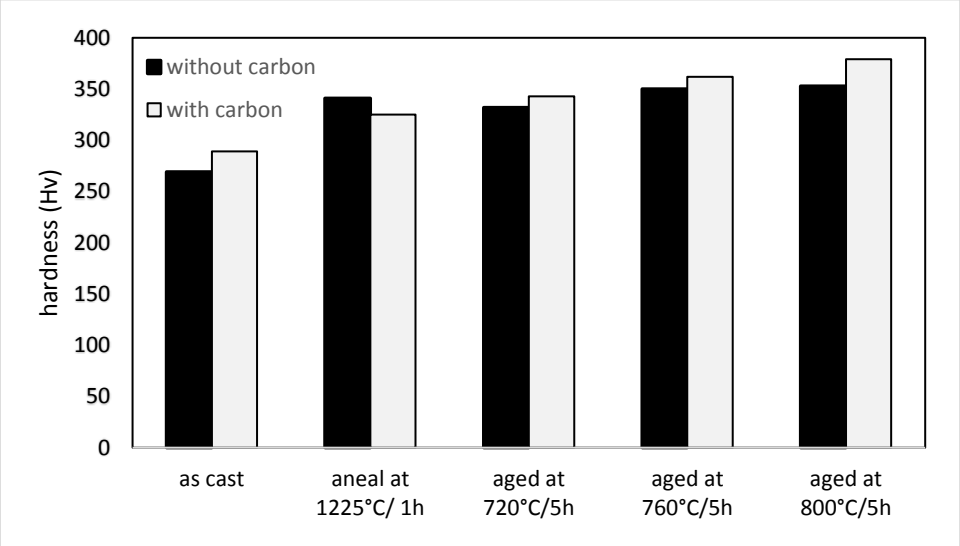

Fig. 7. Hardness values of carbon-free and carbon-containing products in different conditions according to Vickers (VHN).

As can be seen, the hardness value increased owing to the addition of carbon, which led to the formation of carbides in the carbon-containing sample. By aging the sample without the carbon additive at 720 °C, the hardness value increased from 269 HV to 332 HV compared with the as-cast state because of the grain refinement that occurred in the aging state. In both samples, with an increase in the aging temperature from 720 °C to 800 °C, the hardness value increased due to an increase in the amount of the ε-phase by increasing the aging temperature, as could be seen in the XRD results. The reason is that by increasing the aging temperature from 720 °C to 800 °C, the γ→ε transformation was done more, and the ε-phase content increased. The other reason for the increased hardness of the carbon-containing sample was the formation of lamellar $M_{23}C_6$ carbides inside the grains and at the grain boundaries.

3.2. Evaluation of mechanical properties

The results of cold tensile tests of the samples aged at 720, 760, and 800 °C aged for 5 hours for both samples, i.e., without the carbon additive and with the carbon additive, along with the results of casting and annealing at 1225 °C can be seen in Fig. 7.

As shown in this figure, by aging the sample without the carbon additive at 720 °C, the yield strength values increased compared with those of the as-cast state but did not reach the standard level. Moreover, both the tensile strength values and ductility did not change noticeably compared with the values of the as-cast state. With an increase in the aging temperature, one could see a decreasing trend in yield and tensile strength as well as ductility with an increase in the volume fraction of the ε-phase. Thus, in the sample without the carbon additive, not only no improvement was observed in the mechanical properties due to aging but also, according to the precipitate type in this sample (the sigma phase) along with an increase in the volume fraction of the ε-phase, the mechanical properties were degraded, and none of the parameters except ductility and reduction in area reached the standard level.

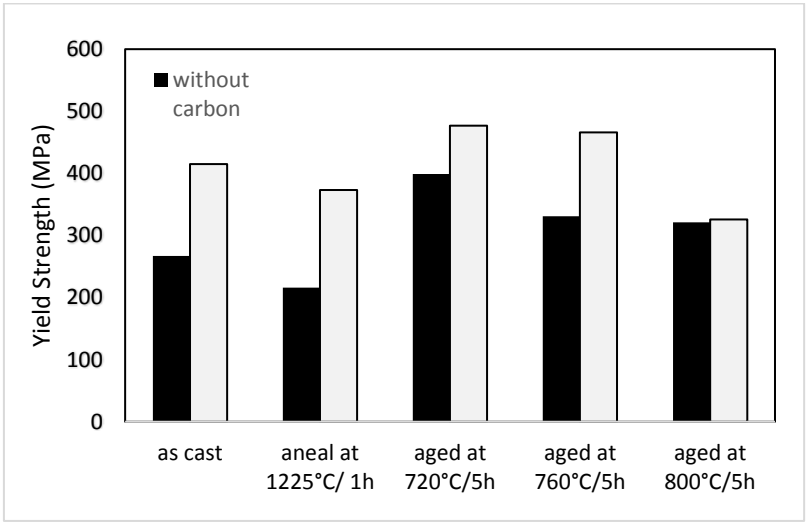

a

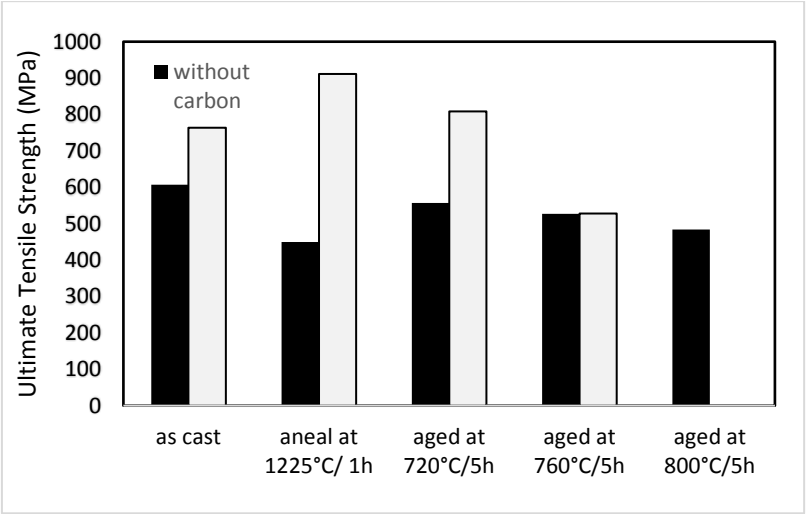

b

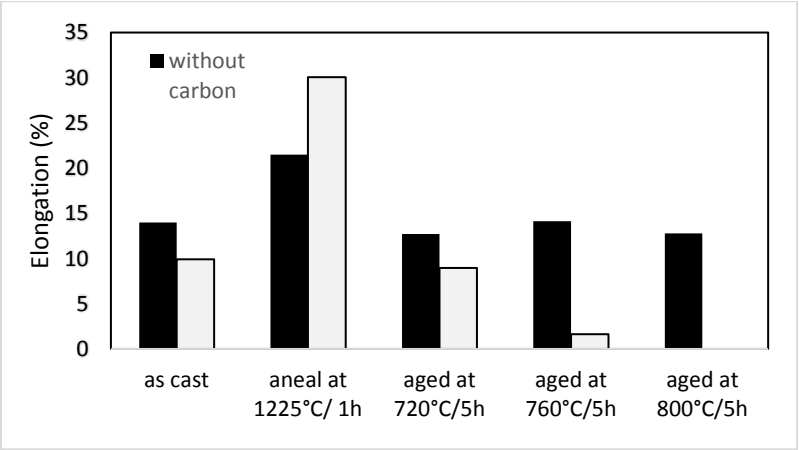

c

Fig. 8. Changes in tensile properties according to aging temperature
a) Yield strength b) Tensile strength c) Elongation percentage

In the sample containing the carbon additive, an improvement in the mechanical properties compared with the as-cast state occurred due to the appropriate distribution of the carbides, which was an expected result. In addition, the yield strength of this alloy increased compared with the as-cast state, considering the precipitates formed in the stacking faults and the distribution of the precipitates inside the grains. However, the ductility decreased because of the formation of the ε-phase and carbides.

Nonetheless, with an increase in the aging temperature, the sample became brittle, and the yield and tensile strength values decreased compared with those obtained in the sample aged at 720 °C owing to the γ→ε transformation at 760 °C and formation of the ε-phase in the structure as well as the formation of interconnected lamellar carbides especially at the grain boundaries. Moreover, the ductility of the alloy reached 1.64%. Therefore, the tensile test results show that in the sample without the carbon additive, a decrease in the mechanical properties in both conditions, i.e., the as-cast and aged conditions, could be observed. This can be ascribed to the absence of carbon in this sample, which led to the absence of carbides in the matrix phase since carbides played a fundamental role in the strengthening of this alloy through precipitation-strengthening. However, in the carbon-containing sample in aging conditions at 720 °C, the mechanical properties were enhanced compared with the as-cast state.

4. Conclusion

1. In the alloy without the carbon additive, due to the single-phase nature of the alloy (HCP), no significant changes were observed in the microstructure by aging at 720°C and 760°C, and the same sigma-phase precipitates that were present in the as-cast and solution annealing state, could be seen in the aging state. However, in the sample aged at 800 °C, the formation of sigma precipitates occurred in the form of parallel lines in HCP1 created by the γ→ε transformation.
2. In the carbon-containing alloy, the sample aged at 720 °C contained fine $M_{23}C_6$ carbides that were distributed inside the grains and at the grain boundaries. With an increase in the aging temperature to 760 °C, parallel lines of the precipitate formation in HCP_1 increased, and a limited number of regions with pearlite-like morphologies could be seen. In addition, the formation rate of lamellar $M_{23}C_6$ carbide, especially at the grain boundaries, increased. The formation of pearlite-like regions at the grain boundaries reached the maximum at the aging temperature of 800 °C.
3. After aging, the γ→ε transformation increased in both samples with an increase in the aging time from 720 °C to 800 °C.
4. In the carbon-containing sample after aging at 720°C, both the ultimate tensile strength (808.9 MPa) and ductility (12.7%) were higher than those of the sample aged at 760 °C due to the presence of a lesser amount of the ε-phase and formation of finer carbides.
5. In the sample without the carbon additive, due to the fundamental role of carbides in strengthening through the precipitation-strengthening mechanism, the absence of carbon and consequently the absence of carbide in the matrix phase of this sample, lower mechanical properties in different conditions of the as-cast and aging were observed.
6. The carbon-containing sample showed the best mechanical properties when aged at 720 °C for 5 hours compared with the other aging temperatures.

5. Refrences

[1] J. B. Park, K. H. Jung, K. M. Kim, Y. Son, J. I. Lee, & J. H. Ryu, Microstructure of as-cast Co-Cr-Mo alloy prepared by investment casting, Journal of the Korean Physical Society, 72, 2018, 947-951. https://doi.org/10.3938/jkps.72.947
[2] R. Silva, M. D. Santos, R. Madureira, et al., Scratch and wear behavior of Co-Cr-Mo alloy in ringer's lactate solution, Materials 16, 2023, 2923. https://doi.org/10.3390/ma16072923
[3] S. Mohammad Moradi, Sh. Zanganeh, Sh. Vardak, R. Bahrami, New Co-Cr-Mo-Nb-Cu alloy for implant applications: properties and chrachterization, Journal of alloys and Compound, 925, 2022, 166387. https://doi.org/10.1016/j.jallcom.2022.166387
[4] Y. Li, Y. Yamashita, N. Tang, B. Liu, S. Kurosu, H. Matsumoto, & A. Chiba, Influence of carbon and nitrogen addition on microstructure and hot deformation behavior of biomedical Co–Cr–Mo alloy, Materials Chemistry and Physics, 135, 2012, 849-854. https://doi.org/10.1016/j.matchemphys.2012.05.069
[5] L. E. R. Vidaurri, M. C. Roman, M. H. Trejo, K.L. F. Chavez, Secondary dendritic arm spacing and cooling rate relationship for an ASTM F75 alloy, Journal of Materials Research and Technology, 19, 2022, 5049-5065. https://doi.org/10.1016/j.jmrt.2022.06.146
[6] A. Mani, & H. F. Lopez, Deformation induced FCC to HCP transformation in a Co–27Cr–5Mo–0.05 C alloy, Materials Science and Engineering: A, 528, 2011, 3037-3043. https://doi.org/10.1016/j.msea.2010.12.024
[7] S. Mineta, S. Namba, T. Yoneda, K. Ueda, & T. Narushima, Precipitates in as-cast and heat-treated ASTM F75 Co-Cr-Mo-C alloys containing Si and/or Mn, Metallurgical and Materials Transactions A, 42, 2011, 1941-1949. https://doi.org/10.1007/s11661-011-0604-4
[8] S. Mineta, S. Namba, T. Yoneda, K. Ueda, & T. Narushima, Changes in microstructure of biomedical Co-Cr-Mo-C alloys with solution treating and aging, Advanced Materials Research, 89, 2010, 377-382 . https://doi.org/10.4028/www.scientific.net%2FAMR.89-91.377
[9] S. H. Lee, N. Nomura, & A. Chiba, Significant improvement in mechanical properties of biomedical

Co-Cr-Mo alloys with combination of N addition and Cr-enrichment, Materials transactions, 2008, 0801150296-0801150296.
https://doi.org/10.2320/matertrans.MRA2007220
[10] M. Chauhan, Microstructural characterization of cobalt chromium (ASTM F75) cubes produced by EBM technique (Master's thesis), 2017.
[11] K. Ozturak, O. Ertugrul, M. Ozcan, Effect of various heat treatments on microstructure and mechanical properties of investment cast Co-Cr-Mo implants, Cumhriyet Science Journal, 42, 2021, 965-976.
https://doi.org/10.1016/j.msea.2022.143380
[12] J. V. Giacchi, O. Fornaro, and H. Palacio, Microstructural evolution during solution treatment of Co–Cr–Mo–C biocompatible alloys, Materials characterization, 68, 2012, 49-57.
https://doi.org/10.1016/j.matchar.2012.03.006
[13] H.Wang, T. Miyagi, A. Chilba, Effect of multiple reverse transformation treatment on grain refinement and mechanical properties of biomedical Co-Cr-Mo-N alloys fabricated by electron beam melting, Materials 16, 2023, 6528.
https://doi.org/10.3390/ma16196528
[14] S. H. Lee, E. Takahashi, N. Nomura, & A. Chiba, Effect of heat treatment on microstructure and mechanical properties of Ni-and C-free Co–Cr–Mo alloys for medical applications, Journal of the Japan Institute of Metals and Materials, 46, 2005, 1790-1793.
https://doi.org/ 10.2320/matertrans.46.1790
[15] S. H. Lee, E. Takahashi, N. Nomura, & A. Chiba, Effect of carbon addition on microstructure and mechanical properties of a wrought Co–Cr–Mo implant alloy, Materials transactions, 47, 2006, 287-290.
https://doi.org/ 10.2320/matertrans.47.287
[16] H. S. Dobbs, & J. L. M. Robertson, Heat treatment of cast Co-Cr-Mo for orthopaedic implant use, Journal of Materials Science, 18, 1983, 391-401.
https://doi.org/10.1007/BF00560627
[17] M. Herrera, A. Espinoza, J. Méndez, M. Castro, J. López, & J. Rendón, Effect of C content on the mechanical properties of solution treated as-cast ASTM F-75 alloys, Journal of Materials Science: Materials in Medicine, 16, 2005, 607-611.
https://doi.org/10.1007/s10856-005-2530-8
[18] ASTM F75-12, Standard Specification for Cobalt-28 Chromium-6 Molybdenum Alloy Castings and Casting Alloy for Surgical Implants (UNS R30075), West Conshohocken, PA: ASTM International, 2012.
[19] ASTM E8/E8M, Standard test methods for tension testing of metallic material, ASTM International, 2010.
[20] B. Geddes, H. Leon, & X. Huang, Superalloys: alloying and performance, Asm International, 2010.
[21] S. Zangeneh, E. Erisir, M. Abbasi, & A. Ramazani, Evaluation of the Aging Effect on the Microstructure of Co-28Cr-6Mo-0.3 C Alloy: Experimental Characterization and Computational Thermodynamics, Metals, 9, 2019, 581.
https://doi.org/10.3390/met9050581
[22] S. Zangeneh, H. R. Lashgari, M. Saghafi, & M. Karshenas, Effect of isothermal aging on the microstructural evolution of Co–Cr–Mo–C alloy, Materials Science and Engineering: A, 527(24-25), 2010, 6494-6500.
https://doi.org/10.1016/j.msea.2010.06.081
[23] D. McParland, S. Baron, S. O'Rourke, D. Dowling, E. Ahearne, & A. Parnell, Prediction of tool-wear in turning of medical grade cobalt chromium molybdenum alloy (ASTM F75) using non-parametric Bayesian models. Journal of Intelligent Manufacturing, 30, 2019, 1259-1270.
https://doi.org/10.1007/s10845-017-1317-3
[24] H. F. López, & A. J. Saldivar-Garcia, Martensitic transformation in a cast Co-CrMo-C alloy, Metallurgical and Materials Transactions A, 39, 2008,8-18.
https://doi.org/10.1007/s11661-007-9370-8